Extraction of City Roads Through Shadow Path Reconstruction Using Laser Data

Pan Zhu, Zhong Lu, Xiaoyong Chen, Kiyoshi Honda, and Apisit Eiumnoh

Abstract

This paper presents an automatic road extraction technique that combines information from aerial photos and laser scanning data (LSD). This innovative Road Extraction Assisted by Laser (REAL) can detect the road edges shadowed by surrounding high objects. A new concept of Associated Road Line (ARL) graph from LSD is introduced to enhance Real Road Line (RRL) graph from aerial photos. The extraction process consists of three steps: The first step is analysing laser images where parameters such as height and edges of high objects are obtained. Secondly, digital images are analysed where road edges are detected. It is evident that ARL and RRL graphs are homeomorphous which provides a theoretical foundation of REAL. The gaps of RRL are bridged through their ARL with a topological transformation. Finally, shadowed parts of RRL are reconstructed by a spline-approximation algorithm. The experimental results show that this approach is effective and has potential advantages.

Introduction

Road extraction from digital images is becoming one of the most attractive research topics in recent years due to tremendous advances in geographic information systems (GIS) and the importance of roads in modern societies. The essential function of a road is to provide a link between places of interest in a geographical region in order to transport resources for human activities. However, this fundamental function of a road has been extended to be an economical and political concept in our civilized societies (Baumgartner, *et al.*, 1997). Recent advances in GIS make it possible to develop a systematic methodology for managing transportation of goods and people in the most efficient and optimal way. Road extraction techniques are an effective tool to collect the required road data for a GIS. Therefore, computer-based road extraction approaches have been extensively studied in past years.

In general, it is relatively easy to extract road information from digital images in a rural areas than in an urban areas. Since most of the roads are built with nearly equal widths (i.e., both of the road edges along the traffic directions are nearly parallel to each other) and the centerlines of the roads have the least curvature variations at each location in order to satisfy the road safety requirements (Gruen and Li, 1997), one can search the edges of any visible road in digital images based on these two geometric characteristics. Roads in a rural areas have more open space around them; thus, the rural roads are seldom shadowed by other tall objects. On the other hand, densities of road objects in an urban area are much higher than those in a rural areas. Therefore, it is most likely that urban roads in digital images are hidden underneath the shadows of other objects, such as tall buildings, trees, road posts, and traffic. It is almost impossible to remove the influence of these shadows using existing road extraction techniques, so automatic road extraction for urban roads under the shadows of other objects remains a great challenge.

Review of current road extraction techniques to deal with non-visible roads in digital images reveals that Semi-Automatic Feature Extraction by Snakes (SAFES) (Trinder and Li, 1995) and "Zip-Lock" snakes (Neuenschwander, *et al.*, 1995) have been developed. SAFES is based on the two assumptions: (1) variable curvatures of the road centerline, and (2) parallel edges along the road traffic directions (i.e., the assumption of equal width). The road edges are first searched on the assumption of equal width. After that, the curvature of the road's centerline is determined with the road edge information in order to keep the road gradient smooth and with minimal variation. SAFES is the best suitable to a road structure with line features. "Zip-Lock" snakes are the modification of SAFES. By adding automatic algorithms for detecting the seed points, "Zip-Lock" snakes have an automatic feature identification instead of the semi-automatic schemes in SAFES. Although SAFES and "Zip-Lock" snakes can extract invisible road information from digital images, they were developed mainly for applications in a rural area, due to a lack of capacity to deal with large objects, such as tall buildings and trees, as shown in Figure 1.

This paper presents an innovative automatic road extraction technique that combines information from digital images and laser scanning data (LSD). Since 3D topography information of an object on the ground can be easily extracted from LSD regardless of the circumstances around the object, that is, weather and shadows of any buildings and/or other objects would not affect the laser scanning altimetry. The proposed approach can recover the hidden road edges in digital images by removing any high objects identified by LSD. The edges of the high objects from LSD are used to define the so-called associated road line (ARL) graph, which can automatically simulate the hidden road edges due to the shadows of the high objects. The topological transformations of homeomorphous mapping and approximate spline algorithm are also adopted in this Road Extraction Assisted by Laser (REAL) data. A discussion on this will be presented in detail as follows.

Pan Zhu, Xiaoyong Chen, and Kiyoshi Honda are with the Space Technology Applications and Research Program, Asian Institute of Technology, P.O. Box 4, Klong Luang, Pathumthani, 12120, Thailand (rsc008397@ait.ac.th).

Zhong Lu is with the Department of Civil Engineering, The University of Hong Kong, Pokfulam Road, Hong Kong.

Apisit Eiumnoh is with the Rural Development, Gender and Resources Program, Asian Institute of Technology, P.O. Box 4, Klong Luang, Pathumthani, 12120, Thailand.

Photogrammetric Engineering & Remote Sensing
Vol. 70, No. 12, December 2004, pp. 1433–1440.

0099-1112/04/7012–1433/$3.00/0

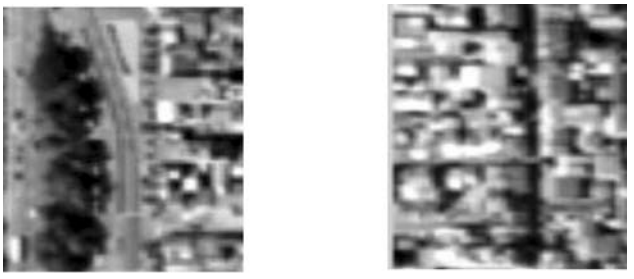

(a) (b)

Figure 1. Roads hidden underneath the shadows of trees (a) and buildings (b).

This paper briefly describes laser scanning data (LSD) and digital image processing. Then, the concepts of Real Road Line (RRL) graph and Associated Road Line (ARL) graph are introduced, and the RRL and ARL graphs are proven to be homeomorphous to each other. After that, formulation and numerical realization of REAL are presented. Finally, the proposed innovative approach of REAL is validated by experimental results.

Laser Scanning Data and Digital Image Processing

Laser scanning is a technology used to measure physical characteristics such as distance, density, velocity, and shape. It is based on sequential range measurement from an airborne sensor to points on the surface. Range is measured with highly collimated laser beam by detection of the turn-around time of laser flight. Knowing the precise position and orientation of the airborne platform from differential GPS and INS measurements, the geographic position of the surface points in three spatial dimensions can be calculated to decimeter accuracy (Sohne, *et al.*, 1993). The periodic deflection of the ranging beam across the direction of flight causes the sampled surface points to be distributed over a strip of 250–500 m width which allows for the generation of surface elevation *images*, i.e., of 2D arrays with elevation data in each cell. Figure 2 shows the laser data and its corresponding 3D reconstruction.

The characteristics of a laser scanner provide a possibility to identify the roads under the shadows and occlusions from buildings and trees.

A digital image can be processed to identify the boundaries of an object, based on changes in gray scale value between the two edges of the boundaries. Road edges may be detected by different gray scale values between road materials and surrounding objects in digital images. Current road edge detection techniques from digital images include the Sobel algorithm, Laplacian of Gaussian (LOG) operator, and the Canny operator (Haralick, 1984). In this paper, the Canny operator is adopted to perform the edge detection from both aerial and laser digital images.

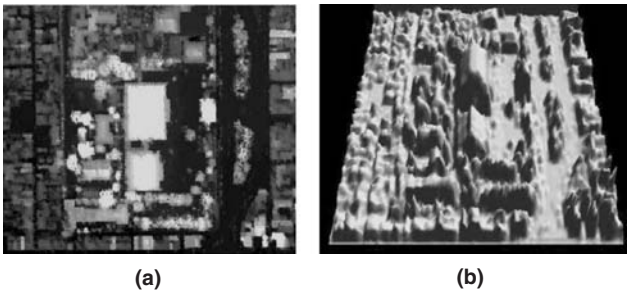

(a) (b)

Figure 2. Laser data (a) and 3D reconstruction (b).

The REAL Approach

ARL Assumption from a Laser Image

Topological Properties of RRL Graph

Roads in modern societies have many topological features that can be used in road extraction. For example, individual roads must be designed to direct traffic in a gradual and smooth way in order to satisfy road safety requirements. Therefore, the curvature variations of an individual road often have the minimum values on its centerline with the maximum allowable slopes. The width of an individual road is usually invariant along the traffic directions except for the intersections of several roads. In addition, urban roads are generally surrounded by high objects, such as, tall buildings and trees, and road surfaces are made of either asphalt or concrete of which spectral characteristics can be easily captured by aerial, digital images. Furthermore, road networks, which are equivalent to the plane networks of topology, may be formed by connecting individual roads in a geographical region. Any individual road in a road network can be regarded as a single path in a topological network (Bredon and Glen, 1993). The so-called path in topology means a graph composed of a sequence of arcs within a finite number. All arcs are different from each other and can be passed through; each arc can be passed only one time. That is, in this sequence of arcs, one of the ends of each arc has must be regarded as the starting point of this arc the other one as its terminal. The common end of two connected arcs must be the terminal of the first arc and the starting of the second arc. Similarly, the terminal of the second arc must be the starting of the third arc, and so on. An end of arc is also termed summit (or top) of network. In this paper, it is not the purpose to go into the whole road network, but instead, a single path within it. A single path is also regarded as a subnetwork of the road network. Now, we will investigate the topological property of any single path in the road network. To do this, we first introduce the concept of "order of summit" (Bredon and Glen, 1993). In topology, the order of summit is understood by the number of ends of arcs situated at the summit under discretion. Obviously, according to the definition of single path, on each of the single paths, the order of any of summits between the starting and terminal of this single path can be equal to an even number, and the order of either of summits at the starting and terminal of this single path, an odd number. The reason is that there are two ends of arcs located at any of middle summits, and only one arc at the starting and terminal of this path, respectively. See Figure 3 for a description of this situation.

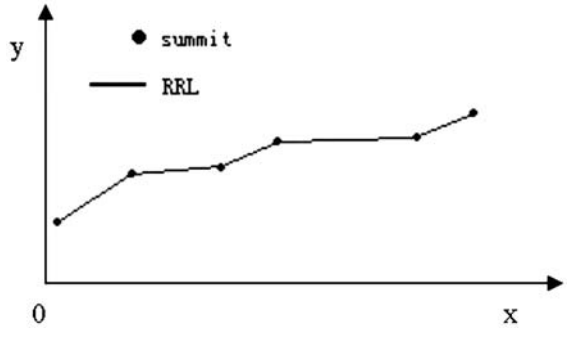

Figure 3. Sketch of distribution summits of RRL graph.

Based on this approach, a conclusion on the topological invariant of single road graph can be drawn as follows:

Theorem 1: Any single road graph has exactly two odd-order summits.

We know from topology (Bredon and Glen, 1993) that the property of a graph exactly having two odd-order summits is nothing but a topological property. This property remains unchanged with all possible homeomorphous mappings to this graph; therefore, it is also called a topological invariant. Homeomorphous mapping is also called a topological transformation i.e., a kind of continuous and bijection operator. This invariant describes the identical property of images of these graphs with respect to all possible homeomorphous mappings. In other words, all graphs are topologically equivalent (homeomorphous) to each other, if and only if, any of them has exactly two odd-order summits. A very interesting aspect is that a straight-line segment $[a, b]$ just has two odd-order summits, located at two ends, a and b, of this segment. According to what was just stated, any single path L in road network should be homeomorphous to any straight-line segment, $[a, b]$. In this way, a single path L may be written in set structure form as follows:

$$L := \{(X, Y); X = X(t), Y = Y(t), \quad t \in [a, b]\}, \tag{1}$$

where (X, Y) is Descartes coordinate point on curve L, and t a parameter. As a matter of fact, Equation 1 gives a definition of homeomorphous mapping F from straight-line $[a, b]$ to graph L as follows:

$$F: [a, b] \to L: \quad t \mapsto (X, Y). \tag{2}$$

As seen, road graph L is nothing else than a simple curve in geometry which is composed of simple arcs whose number is finite.

Associated Road Line (ARL) Graph

It was stated that homeomorphism of two graphs to each other means that they have the same topological invariant. In this case, these two graphs absolutely make no difference to each other from the point of view of topology despite what background or what sources of data they originate. Furthermore, there exists a topological transformation to make these two graphs superimpose. Unfortunately, this theorem is nothing but a pure existential theorem of topological transformation. We can hardly identify this kind of topological transformation in practice. Even so, it will give us a very useful elicitation. When we do a road extraction based on remotely sensed data such as an aerial photo where some parts of a road are occluded by shadows of trees and buildings, we can theoretically use any kind of information coming from the other sources than the aerial photo to assist us with identifying features of the real road. When there is no aerial photo information due to obstruction from shadows, only then, the edge curve is drawn using this kind of ancillary information homeomorphous to RRL graph. However, in this paper we try to use LSD as assistant information in creating the REAL approach. In doing so, what we should do is as follows: to put forward a concept of ARL graph and show the way how to draw it based on LSD; to verify homoemorphous integrity of the ARL graph to the RRL graph. Before doing this, let us discuss the details about LSD.

In the Section on "Laser Scanning Data and Digital Image Processing," we have discussed the attributes of LSD. We know that LSD provides us two kinds of useful information. One is height information which can be used to decrease computing workload and remove false roadways on high objects, so that efficiency of detecting edge of images is signally heightened. The second one is the type of supporting information that we can detect in the circumstances of roadways under shadows of trees and occlusions of high objects. As concern for this kind of information, LSD plays a very crucial assistant role in our REAL. It can be seen that the essential obstacle of road extraction lies in the difficulty of getting at any information of site circumstances for real roads under shadows and occlusions in aerial photos and satellite images. To extract a road by the use of computing technology, the RRL is normally tracked along its gray scale attribute. If tracing of some parts of a road is interrupted by shadows or occlusion and lacking other information for determining the context of these parts, it is indeed impossible for this road extraction to get past these interrupted parts.

In this research on the REAL approach, what we do first is detect road edges by utilizing LSD. Obviously, it is easy to detect edges of high objects such as buildings and trees. Nevertheless, we should see that a laser scanner is one of the altimeters for measuring distance, density, velocity, and shape. It is difficult to make a detection of a road edge line because a road has almost consistent elevation; the gray scale values on both sides of roadside also are nearly equal to each other. Although road information cannot be arrived at directly from LSD, an important fact may be detected from information of edges of buildings, trees, and other high objects on roadsides which is particularly useful for helping us to validate our road extraction approach. In Figure 1a we can see that one side of the road is occluded by the shadows of trees and on the other side there are buildings parallel with the road edge. At the same time, through the LSD we find out that the ground under the shadows is very even, and there are no high objects. On this account, following the principles of road design, we may make a guess that under the shadows must be one side of the road. In this way, we may regard the trees' edges coming from the laser image and associated with the road line together along with this road direction as another kind of road line, i.e., the ARL graph. In order to set up easy computer processing, we set a buffer of the trees' edges, and only extrapolate those lines parallel to the road direction and close to the road (see Figure 4).

Needless to say, the ARL graph and the RRL graph come from quite different image sources. The ARL graph is from LSD, and the RRL graph from aerial photo information. These two kinds of graphs are different between each other in geometric conformation. For instance, the ARL graph, a curve formed by edges of trees, is irregular, and behaves as changing of its curvature in a rapid and sharp way; rather, the RRL graph should be a smooth curve, as changing of its curvature in a slow and exiguous way (see Figure 3). Whether the ARL graph can really play a key assistant role in extracting road approach as indicated above is definitely dependent upon topological

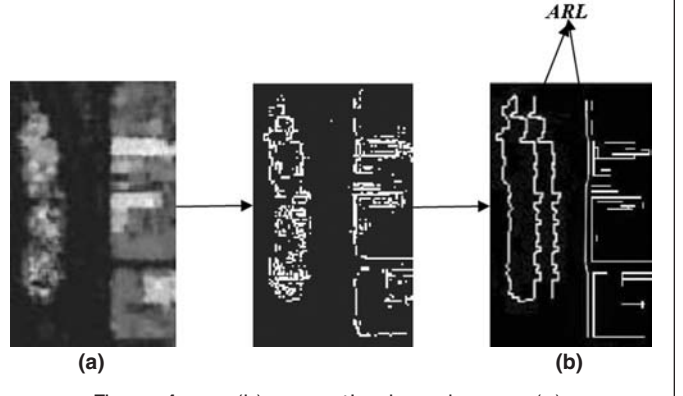

Figure 4. ARL (b) generation based on LSD (a).

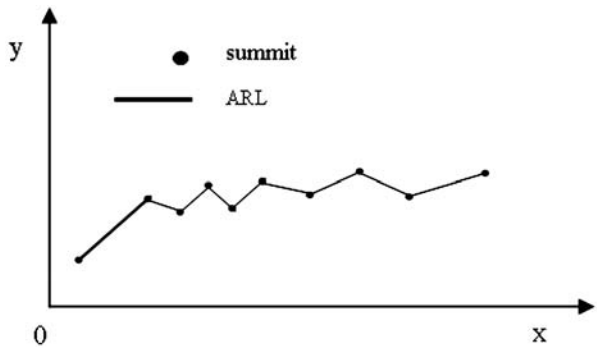

Figure 5. Sketch of distribution of summits of the ARL graph.

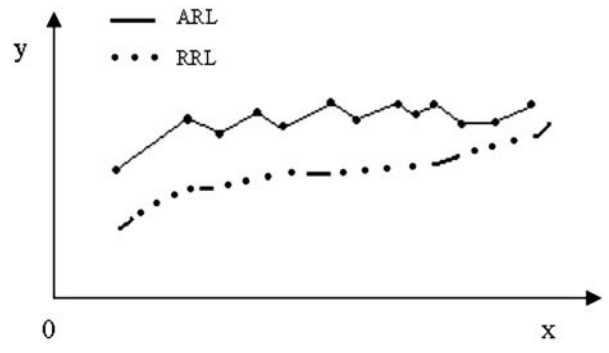

Figure 6. Homoeomorphous integrity of ARL graph *l* to RRL graph *L*.

homoeomorphous integrity of the ARL graph to the RRL graph. Now, let us demonstrate this problem. No matter how rapidly and sharply the curvatures of the ARL graph change, the ARL graph is nothing less than a curve composed of a sequence of arcs whose number is finite. See Figure 5 for a good illustration of this distribution.

Suppose the ARL graph has n arcs; that means it has $n + 1$ summits. It can be seen from Figure 5 that in this case any of summits in between two terminals of the ARL graph is an even-order summit because the number of ends of two arcs situated at this summit is equal to two. For both terminals of the ARL graph, each of summits of them is clearly an odd-order summit because there is only one end of one arc. In this way, we come to the conclusions in the following:

Theorem 2: The ARL graph based on LSD exactly covers two odd-order summits.

Theorem 3: The ARL graph and the RRL graph are homeomorphous to each other.

Thus, it can be seen that in the ARL graph l also is a simple curve in geometry which can be also represented a set structure form as follows:

$$l := \{(x, y);\ x = x(t),\ y = y(t),\quad t \in [a, b]\}, \tag{3}$$

where (x, y) defines the Descartes coordinates of point on the curve l.

The REAL Realization

The Homeomorphous Mapping from ARL to RRL

As mentioned above, if the two graphs have the same topological invariant, then these two graphs are homeomorphous to each other; that is to say, both of these graphs are topologically equivalent to each other. In this case, there theoretically exists unique homoemorphous mapping, making both graphs congruent with each other. However, this mapping cannot be practically found, but then it is also possible and easily to get the numerical representation of this mapping in the circumstances like the graphs of ARL and RRL.

Now, let us examine the numerical representation problem of homeomorphous mapping from RRL graph L to ARL graph l. We suppose these two graphs are already given because L and l are simple curves, and we have their set structure forms as Equations 1 and 2. Following these two equations, we can immediately establish mapping as:

$$H : l \to L : (x, y) \to (X, Y): \tag{4}$$

$$\begin{cases} X = x \\ Y = y - h, \end{cases}$$

where h defines the Euclidian distance from point (x, y) to (X, Y):

$$h = |(x, y) - (X, Y)| = [(x - X)^2 + (y - Y)^2]^{1/2} = y - Y. \tag{5}$$

Therefore, h is a function of the point (x, y) or (X, Y). On the other hand, the inverse H^{-1} of mapping H can be expressed as:

$$H^{-1} : L \to l : (X, Y) \to (x, y): \tag{6}$$

$$\begin{cases} x = X \\ y = Y + h. \end{cases}$$

It is clear from Equations 4, 5, and 6 that H is continuous and bijection mapping. That is to say, we have:

$$\begin{cases} H(l) = L \\ H^{-1}(L) = l. \end{cases} \tag{7}$$

It follows that H is homeomorphous mapping (topological transformation). In the case where both l and L are presented as an image, it is impossible to analytically define H; rather, it can be numerically realized. Attention should be drawn to this theorem as it presents a method to numerically realize the homeomorphous mapping from l to L only on the assumption of knowing both curves l and L. At the same time, this homeomorphous mapping may be understood by a non-uniform stretching motion of l to L in the direction of y-axis to make l congruent with L (See Figure 6).

Formulation and Numerical Realization of REAL

In REAL, the whole ARL graph is given, however, we cannot at first make use of the above-named method for reaching our goal because only several occluded gaps of road are desired to extract with information from aerial photo. In this section, we will describe the problem about how to extract the gaps between two segments with aerial photo information.

Take the Descartes coordinate system O-xy, where the x-axis is as parallel as possible to the RRL graph L desired to extract. Indicate a point on L as (X, Y), and on its ARL graph l as (x, y). For simplicity and without loss of universality, suppose L just has two road segments Δ_1 and Δ_2 with aerial photo information; we write:

$$\Delta = \Delta_1 + \Delta_2. \tag{8}$$

In this case, we have three gaps in L with no aerial photo information, denoted as G_0, G_1 and G_2 respectively which means:

$$L = G_0 + \Delta_1 + G_1 + \Delta_2 + G_2. \tag{9}$$

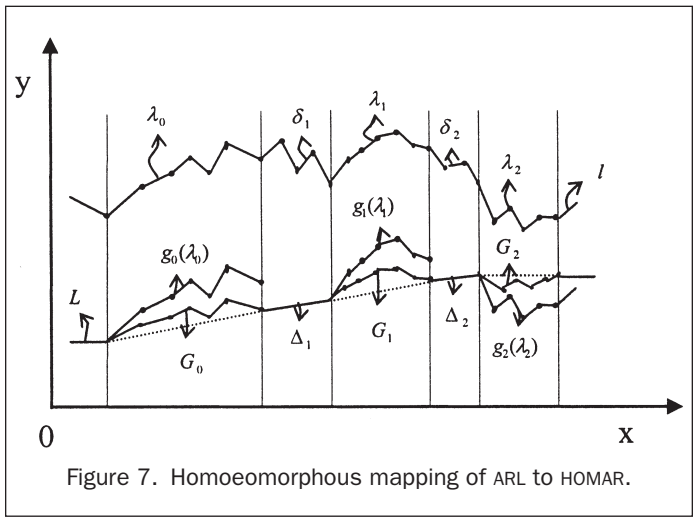

Figure 7. Homoeomorphous mapping of ARL to HOMAR.

See Figure 7 for further details. Now, let the sign *Gap* denote the subset of *L* as:

$$Gap = L - \Delta = G_0 + G_1 + G_2. \tag{10}$$

Suppose we have drawn the ARL graph l from original laser image. At the same time, let δ_j and λ_k denote the projections of Δ_j $(j = 1, 2)$ and G_k $(k = 0, 1, 2)$ on graph l in the direction of y-axis, respectively; we can write:

$$\begin{aligned} \delta &= \delta_1 + \delta_2 \\ \delta^c &= l - \delta = \lambda_0 + \lambda_1 + \lambda_2. \end{aligned} \tag{11}$$

In this way, the formulation of the REAL problem should be reduced to reconstructing information of subset *Gap* of *L*. To do this, we first need to create a homeomorphous mapping H^* from δ to Δ. Following the discussion in Section of "The Homeomorphous Mapping from ARL to RRL" we write:

$$H^* : \delta \to \Delta : (x, y) \to (X, Y): \tag{12}$$

$$\begin{cases} X = x \\ Y = y - h, \end{cases}$$

where h is defined on each point $(x, y) \in \delta$ or $(X, Y) \in \Delta$. Second, we should find an extension of mapping H^* to δ^c, i.e., to determine a mapping $\hat{H}$ defined in the domain l and its restriction on δ is equal to H^*. That means $\hat{H}$ is equal to H^* if all points $(x, y) \in \delta$:

$$\hat{H} = H^* : \delta \to \Delta : (x, y) \to (X, Y): \tag{13}$$

$$\begin{cases} X = x \\ Y = y - h. \end{cases}$$

We know from functional analysis (Hu, 2001) that there originally does not exist a unique extension $\hat{H}$ of mapping H^* to δ^c because of inverse space of mapping $\hat{H}$ being much *larger* than its image space.

Now, we will determine a required extension of $\hat{H}$. For this, we should proceed as follows. Consider Figure 7 and be concerned with the subset λ_0 of the ARL graph l. We take a shifting operator g_0 such as:

$$g_0 : \lambda_0 \to g_0(\lambda_0) : (x, y) \to (X^0, Y^0): \tag{14}$$

$$\begin{cases} X^0 = x \\ Y^0 = y - h_0, \end{cases}$$

where h_0 means the distance from the starting (X_0, Y_0) of the RRL to the starting (x_0, y_0) of the ARL graph. Curve $g_0(\lambda_0) := \{(X^0, Y^0)\}$ is the image of curve λ_0 with respect to operator g_0 (see Figure 8).

Next, we define an operator:

$$f_0 : g_0(\lambda_0) \to G_0 : (X^0, Y^0) \to (X, Y): \tag{15}$$

$$\begin{cases} X = X^0 \\ Y = Y_G^0 + D^0, \end{cases}$$

where Y_G^0 is equal to vertical coordinate of intersection (X^0, Y_G^0) of straight line $x = X^0$ with straight line connecting the start (X_0, Y_0) and terminal (X_1, Y_1) of G_0, and D^0 is a directional and perpendicular distance from a point $(X^0, Y^0) \in g_0(\lambda_0)$ to the chord connecting point $(X_0, Y_0) \in G_0$ with point $(X_1^0, Y_1^0) \in g_0(\lambda_0)$. If the curve $g_0(\lambda_0)$ is up the straight line from (X_0, Y_0) to (X_1, Y_1), D^0 is taken as positive; otherwise, it is a negative. In this way, Equations 14 and 15 are defined as a composite operator λ_0:

$$(f_0 \circ g_0) : \lambda_0 \to G_0 : (x, y) \to (X, Y): \tag{16}$$

$$\begin{cases} X = X^0 \\ Y = Y_G^0 + D^0. \end{cases}$$

Proceeding similar to this for gaps G_1 and G_2, we can write for all graphs G_j $(j = 0, 1, 2)$ as follows:

$$(f_j \circ g_j) : \lambda_j \to G_j : (x, y) \to (X, Y): \tag{17}$$

$$\begin{cases} X = X^j \\ Y = Y_G^j + D^j, \end{cases}$$

where the definitions of Y_G^j and D^j $(j = 1, 2)$ are similar to Y_G^0 and D^0. Up to now, we can write the extension $\hat{H}(l)$ of mapping H^* to δ^c as follows:

$$\hat{H} = \begin{cases} H^* & on \quad \delta \\ (f_j \circ g_j) & on \quad \delta^c, \end{cases} \tag{18}$$

where operators H^* and $(f_j \circ g_j)$ are defined as Equations 13 and 17. It is easy to prove that mapping $\hat{H}$ is a continuous and bijection mapping, i.e., its image $\hat{H}(l)$ is a curve homeomorphous to both ARL graph l and RRL graph L. For an easy understanding, we take a look at the sketch map in Figure 8, and we can find $\hat{H}(l)$ that is a curve with a simple structure which is composed of a sequence of a limited number of arcs and just two odd-order summits at the starting and terminal of the RRL graph. At the same time, we can see that on δ_j curve $\hat{H}(l)$ is absolutely congruent with segment Δ_j $(j = 1, 2)$ of the RRL graph with aerial photo information, and on δ^c, represents gaps G_j $(j = 0, 1, 2)$. Therefore, $\hat{H}(l)$

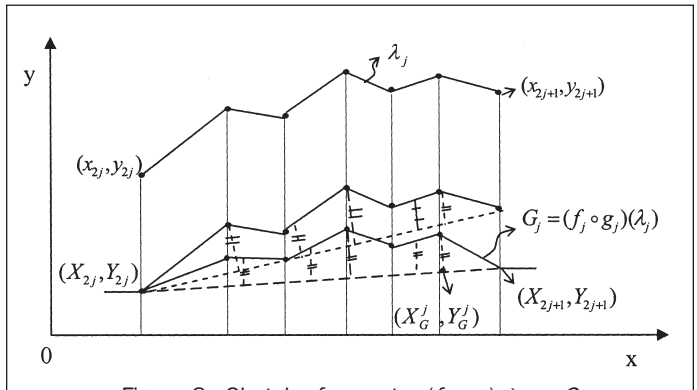

Figure 8. Sketch of operator $(f_j \circ g_j)$: $\lambda_j \to G_j$.

is called the homeomorphism-matching of incomplete RRL graphs from complete ARL graphs (HOMAR).

Although the HOMAR $\hat{H}(I)$ may not be as smooth as the original incomplete RRL graphs, the approximate spline algorithms can be used to correct the irregular HOMAR $\hat{H}(I)$. In this study, the Cardinal spline algorithm is adopted, where the spline curves are always represented by a three-order polynomial transform with one or two-order continuous derivations. It is worth pointing out that the Cardinal spline algorithm in REAL can be automatically executed because the seeds for the algorithm are randomly selected from the complete ARL graphs that are obtained from the discrete LSD.

Experimental Validation of REAL

The proposed innovative approach of REAL in this paper has been validated by an experiment that involves the task of road extraction for an urban area. The experiment is divided into four main steps.

First, the aerial photo and laser scanning image for the area were filtered with an adaptive filtering technique in order to eliminate noises as much as possible.

Second, the last attribute, amplitude or reflectance registration, provides radiometric information about the surveyed area. The reflectance can be seen as an *image* in a very narrow wave-length band which can be used in a classification algorithm, e.g., separating paved areas from height (Figure 9a). The processing of laser data is often directed at either removing unwanted measurements either in the form of erroneous measurements or subjects or modeling data given a specific model. Removing unwanted measurements, as in the case of finding a ground surface from a mixture of ground and vegetation measurements is in this context referred to as *filtering*. The unwanted measurements can, depending on application, be characterized as noise, outliers, or gross errors. Finding a specific geometric or statistic structure, as buildings or ground, is referred to as *classification*. The generalization, finally, of the classified objects is referred to as *modeling*. Hence, filtering, classification, and modeling are defined according to goals and not to method. Examples of the classification can be seen in Figure 9b.

Third, the road edge detections by the Canny operator and edge refinement based on morphological post processing were conducted to create real road line (RRL) graph and associate road line (ARL) graph. Canny operator has been introduced in the section on "Laser Scanning Data and Digital Image processing." Morphological image processing is a type of processing in which the spatial form or structure of objects within an image is modified. Dilation, erosion, and skeletonization are three fundamental morphological operations. Through some morphological processing, such as erosion, dilation, opening and thinning, the edge map has been improved, and has become available to our research. Figure 10 presents the courses of morphological processing to an edge map.

Fourth, selection of ARL is conducted. We have known the theory on ARL graph from laser data which is applied to road extraction from remotely sensed data. As far as two graphs have the same topological invariant, they can be regarded as homeomorphous maps each other. Hence, there exists a topological transformation that makes these two graphs superpose upon each other. In this case, we have to select the ARL first, which is possible for the reconstruction of shadow path in aerial photograph. Normally, all edges of buildings and trees are possible to become ARL if only the roads nearby them are under the shadow of buildings and trees. In fact, it is rather easy to implement our operation. In Figure 11, the left edges of the buildings are the requirements of ARL selection. We simply set a buffer for all building edges as our first step, and keep the left-side lines as needed (see Figure 11a). In order to improve the lines' quality, the Cardinal spline algorithm is utilized for linking these line segments (see Figure 11b).

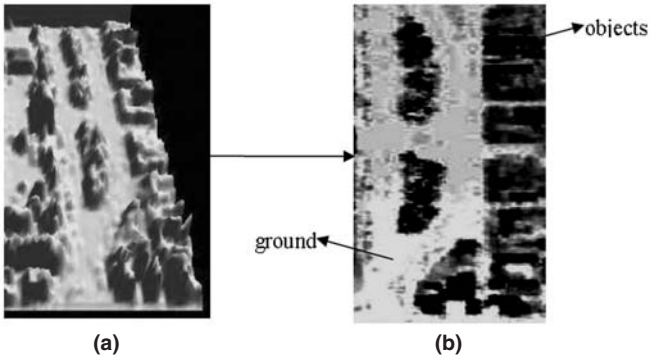

Figure 9. Perspective views of elevations (a), and separating ground and objects (b).

As shown in Figure 12, the road extraction results for the aerial photos fail to identify the road edges under the shadows of trees which make the detected road much wider than reality. On the other hand, the road extractions from REAL demonstrates promising results that can be further processed to deal with more complicated applications such as urban roads with traffic and road markers and barriers.

Conclusions

This paper presented an automatic road extraction technique that combines information from aerial photos and laser scanning data (LSD). This novel Road Extraction Assisted by Laser (REAL) can detect the road edges shadowed by surrounding high objects, such as tall buildings and trees. A new concept of Associated Road Line (ARL) graphs from LSD is introduced to enhance Real Road Line (RRL) graphs from aerial photos. It is evident that ARL and RRL graphs are homeomorphous to each other which provides a solid theoretical foundation of REAL. The gaps in incomplete RRL graphs due to the shadowed road edges are bridged by complete ARL graphs through a unique homeomorphous mapping $\hat{H}$, that can be determined by a two-step approach proposed in this paper. The homeomorphism-matching of incomplete RRL graphs from complete ARL graphs (HOMAR) can be automatically smoothed to match the original incomplete RRL graphs by the built-in Cardinal spline algorithm in REAL. The proposed REAL approach has been validated by experimental results for which manual operation may be involved to remove some false roads due to *noise* in the image processing algorithm of REAL.

References

Baumgartner, A., W. Eckstein, H. Mayer, C. Heipke, and H. Ebner, 1997. Context supported road extraction, *Automatic Extraction of Man-Made Objects from Aerial and Space Images* (*II*) (A. Gruen, E. Baltsavias, and O. Henricsson, editors), Birkhauser Verlag Basel, pp. 299–308.

Bredon, Glen E., 1993. *Topology and geometry*, Springer-Verlag, New York, 350 p.

Castleman, Kenneth R., 1996. *Digital Image Processing*, Prentice Hall, Inc., 667 p.

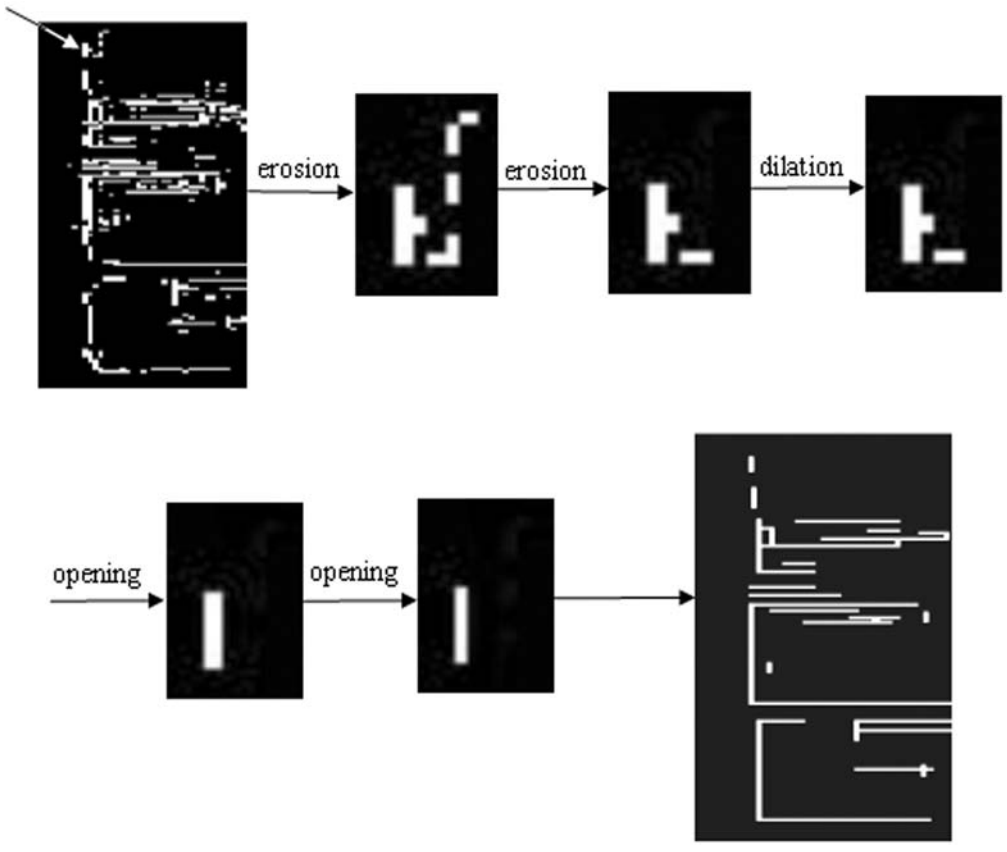

Figure 10. Morphological processing for edge map.

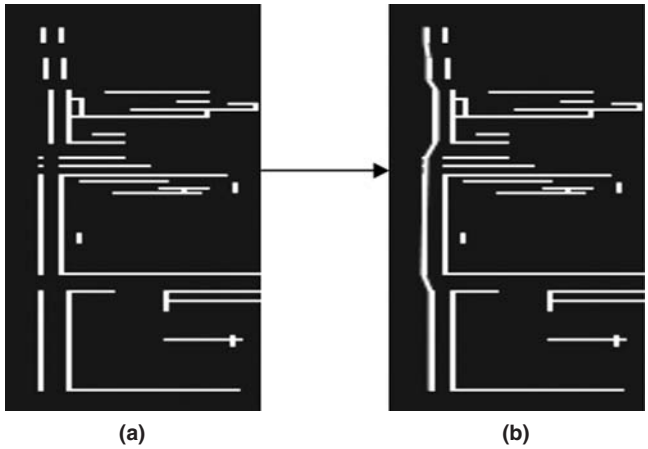

(a) (b)

Figure 11. Selection of ARL with Cardinal spline algorithm: (a) setting the buffer of building edges, and (b) linking the line segments with the Cardinal spline algorithm.

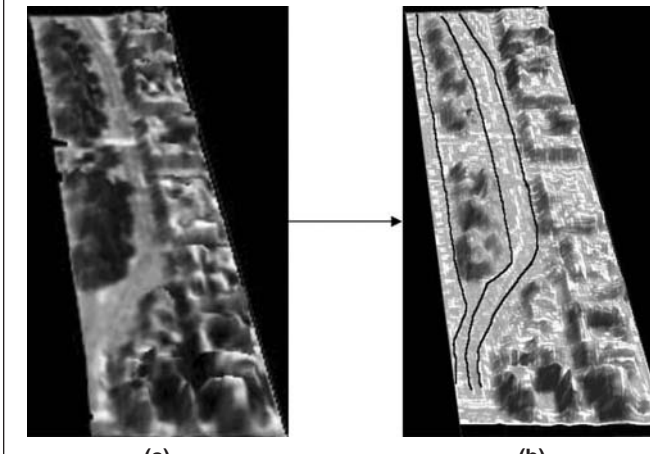

(a) (b)

Figure 12. Roads extracted (b) from 3D image (a) based on REAL.

Gruen, A., and H.H. Li, 1997. Semi-automatic liner feature extraction by dynamic programming and LSB-snakes, *Photogrammetric Engineering & Remote Sensing*, 63(8), pp. 985–995.

Haralick, R.M., 1984. Digital step edge from zero-crossing of second directional derivatives, *IEEE Transactions on Pattern Analysis and Machine Intelligence*, 6(1):58–68.

Hu, S.G., 2001. *Functional Analysis*, China Higher Education Press Beijing and Springer-Verlag Berlin Heidelberg, 296 p. (in Chinese).

Neuenschwander, W., P. Fua, G. Szekely, and O. Kubler, 1995. From ziplock snakes to Velcro™ surfaces, *Automatic Extraction of Man-Made Objects from Aerial and Space Images* (A. Gruen, O. Kubler, and P. Agouris, editors), Birkhauser Verlag Basel, pp. 105–114.

Sohne, W., O. Heinze, C. Hug, and U. Kalberer, 1993. Positioning and orientation of a laser/radar-altimeter survey flight with GPS and INS, *Proceedings of the Gyro Symposium*, Stuttgart, pp. 203–212.

Trinder, J., and H.H. Li, 1995. Semi-Automatic Feature Extraction by Snakes, *Automatic Extraction of Man-Made Objects from Aerial and Space Images* (A. Gruen, O. Kubler, and P. Agouris, editors), Birkhauser Verlag Basel, pp. 95–104.